Spin-Polarization-Induced Structural Selectivity in Pd_3X and Pt_3X ($X=3d$) Compounds

Z. W. Lu,[1] Barry M. Klein,[1] and Alex Zunger[2]
[1]*Department of Physics, University of California, Davis, California 95616*
[2]*National Renewable Energy Laboratory, Golden, Colorado 80401*
(Received 20 December 1994)

Spin polarization is known to lead to important *magnetic* and *optical* effects in open-shell atoms and elemental solids, but has rarely been implicated in controlling *structural* selectivity in compounds and alloys. Here we show that spin-polarized electronic structure calculations are crucial for predicting the correct $T = 0$ crystal structures for Pd_3X and Pt_3X compounds. Spin polarization leads to (i) stabilization of the $L1_2$ structure over the $D0_{22}$ structure in Pt_3Cr, Pd_3Cr, and Pd_3Mn, (ii) stabilization of the $D0_{22}$ structure over the $L1_2$ structure in Pd_3Co, and (iii) ordering (rather than phase separation) in Pt_3Co and Pd_3Cr. The results are analyzed in terms of first-principles local spin density calculations.

PACS numbers: 61.66.Dk, 71.20.Cf, 75.50.Cc

Crystal structure compilations [1,2] reveal that the most commonly occurring structures among intermetallic binary compounds with a 3:1 stoichiometry (A_3B) are the cubic $L1_2$ and the tetragonal $D0_{22}$ (Fig. 1). The crystallographic difference between the $L1_2$ and $D0_{22}$ structures is rather subtle: The two structures have identical *first* neighbor coordination (each A has $8A + 4B$ neighbors and each B has $12A$ neighbors), while a difference exists in the *second* shell (see Fig. 1). The manner in which particular A_3B compounds select the $L1_2$ or the $D0_{22}$ configuration appears to be rather interesting. For example [2], the $4d$ trialuminides Al_3M show the sequence $L1_2 \rightarrow L1_2 \rightarrow D0_{22}$ as M varies across the $4d$ row Y $\rightarrow$ Zr $\rightarrow$ Nb, while the $3d$ palladium alloys Pd_3X show $L1_2 \rightarrow L1_2 \rightarrow D0_{22} \rightarrow L1_2 \rightarrow L1_2 \rightarrow L1_2$ as one proceeds in the $3d$ row X = Sc $\rightarrow$ Ti $\rightarrow$ V $\rightarrow$ Cr $\rightarrow$ Mn $\rightarrow$ Fe [3] (for X = Co and Ni, the systems phase separate). The origin of such regularities was the subject of numerous investigations including the d-electron "generalized perturbation method" (GPM) [4], and first-principles calculations [5–7]. However, these calculations failed to reproduce the observed structural trends. These calculations were nonmagnetic (NM), i.e., without spin polarization. This appeared to be a reasonable assumption, since one expects that an alloy rich in a nonmagnetic component (e.g., Pd_3Cr) or one without any magnetic components (e.g., Pd_3V) will not have any significant magnetic effects. We demonstrate here that spin polarization has a crucial influence on the structural stability of Pd_3X and Pt_3X compounds: It stabilizes the observed $L1_2$ structure over the $D0_{22}$ structure in Pt_3Cr, Pd_3Cr, and Pd_3Mn, the $D0_{22}$ structure over the $L1_2$ structure in Pd_3Co, and is responsible for compound formation (rather than phase separation) in Pt_3Co and Pd_3Cr.

The key insight to stability in compounds and alloys has traditionally been the association of stability with low density of states (DOS) at the Fermi energy E_F [8]. Nicholson *et al.* [5] noted that for transition metal aluminides the more stable of the two structures ($L1_2$ or $D0_{22}$) corresponds to the one with smaller DOS at the Fermi level $N(E_F)$. Local density approximation (LDA) [9] band structure and total energy calculations [6,7] have later substantiated this relation. To examine such a relation for intertransition metal A_3B compounds rather than aluminides we have calculated $N(E)$ (Fig. 2) and total energy difference $\delta E = E(L1_2) - E(D0_{22})$ [Fig. 3(a) and Table I] for Pd_3X with $3d$ atom X = Sc through Cu using the NM linearized augmented plane wave (LAPW) method [10]. We see that the structure with the lower calculated NM total energy (Table I) indeed has a lower calculated NM $N(E_F)$ (Fig. 2), thus substantiating earlier trends for aluminides [5–7]. For example, for Pd_3X with X = V, Cr, and Mn, the Fermi energy, E_F, falls near a DOS *maximum* for $L1_2$ but near a DOS *minimum* for $D0_{22}$; correspondingly, $E(D0_{22})$ is lower than $E(L1_2)$. Unfortunately, while the magnitude of $N(E_F)$ is indicative of the stability of the *calculated* structure, these nonmagnetic calculations incorrectly predict the *observed* stable crystal structure in several cases: While Pd_3V is correctly predicted to be more stable in the $D0_{22}$ structure, the *observed* [2] stable structure for Pd_3Cr, Pd_3Mn [3], and Pd_3Fe is the $L1_2$ structure, not the

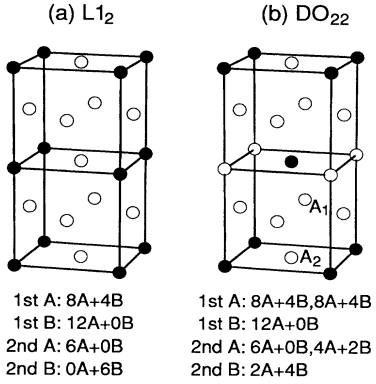

FIG. 1. The crystal structures of the (a) $L1_2$ and (b) $D0_{22}$ structures. The inset shows the atomic coordination about A and B sites in the first (1st) and second (2nd) atomic shells. A_1 and A_2 indicate two distinct A sites in the $D0_{22}$ structure.

 0031-9007/95/75(7)/1320(4)$06.00

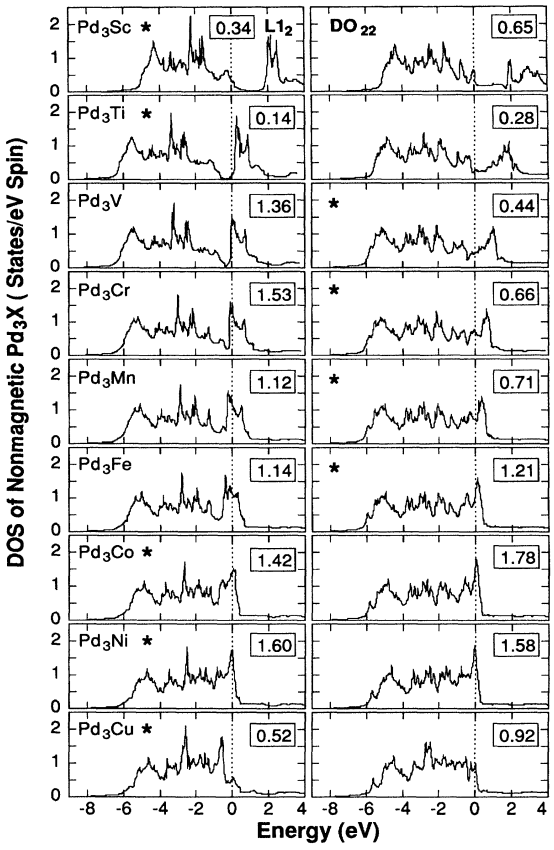

FIG. 2. LDA calculated *NM* total DOS for Pd_3X in the $L1_2$ and $D0_{22}$ structures. The insets denote $N(E_F)$. An asterisk denotes the more stable structure predicted by total energy calculations in the absence of magnetic ordering. Note that the more stable structure has a lower $N(E_F)$.

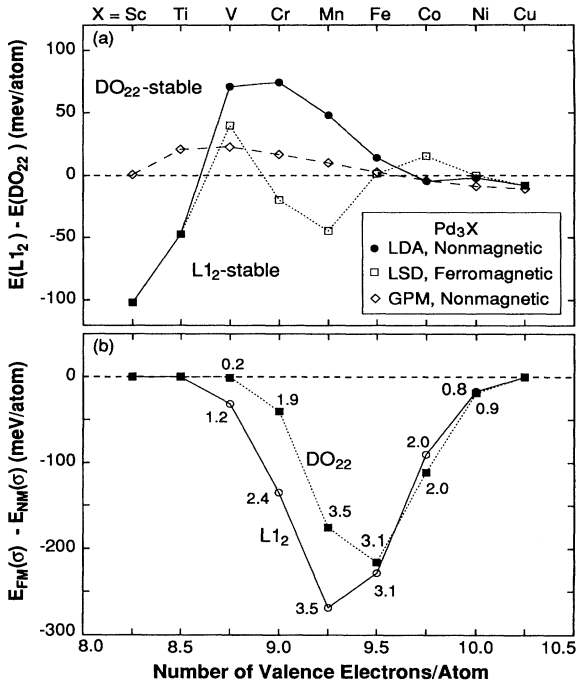

FIG. 3. (a) LDA (present) and GPM (Ref. [4]) calculated energy difference $\delta E = E(L1_2) - E(D0_{22})$ [Eq. (2)] for Pd_3X compounds. Note the reversal of sign for δE due to spin polarization for Pd_3Cr, Pd_3Mn, and Pd_3Co (nearly so for Pd_3Fe). Part (b) gives the magnetization energies $\delta M(\sigma) = E_{FM}(\sigma) - E_{FM}(\sigma)$ [Eq. (3)] for $\sigma = L1_2$ (empty circles) and $\sigma = D0_{22}$ (solid squares) structures and shows the local magnetic moment for the X atom (numbers above or below the symbols).

nonmagnetically predicted $D0_{22}$ structure. Thus, while the correlation between the *calculated* quantities $N(E_F)$ vs $E(L1_2) - E(D0_{22})$ holds, it leads to incorrect predictions for the stability of Pd_3Cr, Pd_3Mn, and Pd_3Fe. The generalized perturbation method calculations [4], based on similar DOS arguments [diamond symbols in Fig. 3(a)] likewise predict Pd_3Cr, Pd_3Mn, and Pd_3Fe (and even Pd_3Sc and Pd_3Ti) to be stable in the $D0_{22}$ structures, in conflict with experiment [2].

In this paper we explain this puzzle by noting that, while a large $N(E_F)$ indeed implies a *destabilizing* factor for the one-electron ("band") energy, it also leads (in open-shell systems) to spin polarization and magnetic moment formation which, in turn, is a *stabilizing* factor. Thus despite their large $N(E_F)$ in the $L1_2$ structure (suggesting one-electron *instability*), Pt_3Cr, Pd_3Cr, and Pd_3Mn (nearly so for Pd_3Fe) are correctly predicted to be more stable in this structure once *spin-polarized* total energy calculations [11] are done. Thus magnetic ordering changes the predictions of NM total energy calculations and restores agreement with experiment.

We have calculated the total energies of Pd_3X, for X = Sc through Cu as well as Pt_3Cr and Pt_3Co in the $L1_2$ and $D0_{22}$ structures using the LDA in both the spin-polarized and spin-unpolarized versions [12] of the full-potential LAPW method [10]. In order to accurately obtain the small energy difference between two fairly similar crystal structures, the calculations were carried out consistently using the same muffin-tin radii R_{MT} and basis set energy cutoffs K_{max}. The Brillouin zone summations were done using the geometrically equivalent **k**-point sampling scheme [13(a)], in which 20 (40) **k** points in the irreducible zone for the $L1_2$ ($D0_{22}$) structure is mapped into the same 60 special **k** points [13(b)] in the fcc structure. We optimized the total energy as a function of volume, as well as the c/a ratio in the $D0_{22}$ structure. The estimated LAPW error for the $E(L1_2) - E(D0_{22})$ energy difference is ~5 meV/atom, and the neglected zero-point energy difference between the two similar structures should be even smaller.

At zero temperature, the *absolute stability of a compound in a structure* σ with respect to phase separation is given by its formation enthalpy $\Delta H(\sigma)$

$$\Delta H_\alpha(\sigma) = E_\alpha(\sigma) - x_A E_A(V_A) - x_B E_B(V_B), \quad (1)$$

where $E_A(V_A)$ and $E_B(V_B)$ are the energies of the constituents A and B in their respective ground states (e.g., for Pd_3Ni, it is nonmagnetic fcc for Pd and ferromagnetic fcc

TABLE I. LDA calculated total energy difference (in meV/atom) $\delta E = E(L1_2) - E(D0_{22})$ and the ferromagnetic (FM) DOS at Fermi energy $N(E_F)$ (in states/eV spin) for the $L1_2$ and $D0_{22}$ structures. Note that the spin polarization (included in the FM state) reverses the relative stability of nonmagnetic (NM) $L1_2$ and $D0_{22}$ structures for those compounds marked by an asterisk, thus restoring agreement with experiment [2,3]. PS denotes phase separation.

	Expt. structure	δE_{NM}	δE_{FM} $L1_2$	$N_{\mathrm{FM}}(E_F)$ $D0_{22}$	$N_{\mathrm{FM}}(E_F)$
Pd_3Sc	$L1_2$	−102	−102	0.34	0.65
Pd_3Ti	$L1_2$	−48	−48	0.14	0.28
Pd_3V	$D0_{22}$	71	40	0.64	0.38
Pd_3Cr*	$L1_2$	74	−20	0.57	0.60
Pd_3Mn*	$L1_2$	48	−45	0.59	0.80
Pd_3Fe	$L1_2$	14	1	0.42	0.34
Pd_3Co*	PS	−5	15	0.79	0.46
Pd_3Ni	PS	−2	0	0.95	0.93
Pd_3Cu	$L1_2$	−8	−8	0.52	0.92
Pt_3Cr*	$L1_2$	71	−23	0.56	0.54
Pt_3Co	$L1_2$	−11	−16	0.66	0.65

for Ni), $E_\alpha(\sigma)$ is the energy of structure σ, and α = NM or FM denotes whether structure σ is in the nonmagnetic or ferromagnetic state. The *relative stability of two different ordered structures* is

$$\delta E_\alpha = E_\alpha(L1_2) - E_\alpha(D0_{22}), \tag{2}$$

while the *magnetic stabilization energy of a given structure* σ ($L1_2$ *or* $D0_{22}$) is

$$\delta M(\sigma) = E_{\mathrm{FM}}(\sigma) - E_{\mathrm{NM}}(\sigma). \tag{3}$$

Table I and Fig. 3(a) give δE_{NM} and δE_{FM}, while Fig. 3(b) shows the magnetic stabilization energies $\delta M(L1_2)$ and $\delta M(D0_{22})$, and the local magnetic moment μ_X on the X atom calculated numerically within the muffin-tin sphere (the value of μ_X is rather insensitive to the small change in muffin-tin radius). Table II gives the formation enthalpies $\Delta H_\alpha(L1_2)$ and $\Delta H_\alpha(D0_{22})$ for several systems. Figure 2 depicts the NM total DOS for Pd_3X, where X = Sc → Cu, in the $L1_2$ (left panel) and $D0_{22}$ structures (right panel). One notices the following.

(i) In contrast to the very similar DOS for the $L1_2$ and $D0_{22}$ structures and the small energy difference $E(L1_2) - E(D0_{22}) \sim 20$ meV/atom predicted by the GPM [4], one sees from Fig. 2 a marked difference of the DOS in the $L1_2$ and $D0_{22}$ structures. (a) While the DOS of the cubic $L1_2$ structure resembles that of fcc Pd, having three major peaks, the DOS of the $D0_{22}$ structure are more smeared, reflecting a loss of cubic symmetry in the $D0_{22}$ structure. (b) The DOS of the more stable $L1_2$ structure for Pd_3Sc and Pd_3Ti shows a "pseudogap" near the Fermi level absent in the $D0_{22}$ structure. (c) In the $L1_2$ structure, the Fermi level of Pd_3V, Pd_3Cr, and Pd_3Mn falls on a DOS peak (made mostly of d orbitals of the X atom), while in the $D0_{22}$ structure the Fermi level falls on a relatively flat portion of the DOS. Indeed, these materials are more stable in the $D0_{22}$ structure in a NM LDA description. As a result of these differences, the values of $N(E_F)$ (given in the insets of Fig. 2) and its shape near the Fermi level are strikingly different for the $L1_2$ and $D0_{22}$ structures.

(ii) The above noted trends in the NM $N(E_F)$ induce a concomitant magnetic stabilization energy δM [Fig. 3(b)]: A *larger* energy stabilization δM due to spin polarization relates to a *larger* $N(E_F)$ and with a *larger* localized magnetic moment μ_X on the X atom [Fig. 3(b)]. For example, while the Pd_3X compounds with X = Sc, Ti, and Cu are nonmagnetic (so $\delta M = 0$), when X = Mn and Fe, one sees in Fig 3(b) large energy lowering due to spin polarization ($\delta M \sim -200$ meV/atom), and concomitantly large magnetic moments of $3.5\mu_B$ (X = Mn) and $3.1\mu_B$ (X = Fe) in both the $L1_2$ and $D0_{22}$ structures (as a comparison, bcc Fe has a magnetic moment value of only $2.2\mu_B$). Thus spin polarization induces a local magnetic moment on the "magnetic" $3d$ atoms with large NM $N(E_F)$, while lowering the total energy of the compound. In the case of Pt_3Cr in the $L1_2$ structure for which previous calculation exists, our calculated total magnetic moment in the unit cell ($2.6\mu_B$) agrees with a previous calculation [14] of $2.6\mu_B$ and with the experimental value [15] of $2.5\mu_B$.

(iii) In the NM calculations, Pd_3V and Pd_3Cr have large DOS peaks at E_F in the $L1_2$ structure, and are concomitantly less stable in this structure than in the low $N(E_F)$ $D0_{22}$ structure. However, as spin polarization is introduced, the large DOS peak of the $L1_2$ structure splits, so that E_F now resides in a low DOS region. This leads, simultaneously, to the formation of larger magnetic moments on V and Cr in the $L1_2$ structure relative to the $D0_{22}$ structure. This selective magnetization thus lowers the energy of the $L1_2$ structure more significantly than in the $D0_{22}$ structure [Fig. 3(b)].

(iv) Table I shows that the more stable of the two structures generally (and weakly) relates to a smaller value of the *ferromagnetic* DOS at the Fermi level $N_{\mathrm{FM}}(E_F)$. Thus the trend of total energy stability with $N(E_F)$ does exist, but for the spin-polarized quantities.

(v) The magnetic stabilization energy δM reverses the relative stability predicted by NM calculations in several cases: Spin polarization stabilizes the experimentally observed [2] $L1_2$ structure of Pd_3Cr, Pd_3Mn, and Pt_3Cr (nearly so for Pd_3Fe) over the $D0_{22}$ structure, while for Pd_3Co spin polarization makes the $D0_{22}$ structure more

TABLE II. Nonmagnetic (NM) and ferromagnetic (FM) formation enthalpies, ΔH [in meV/atom, Eq. (1)], of some compounds. ΔH's are taken with respect to the NM fcc Pd, Pt, FM fcc Ni, FM fcc Co, and anti-FM bcc Cr, respectively.

	$\Delta H(L1_2)$		$\Delta H(D0_{22})$	
	NM	FM	NM	FM
Pd_3Cr	126	−9	51	11
Pd_3Co	155	64	160	49
Pd_3Ni	61	43	62	44
Pt_3Cr	−68	−185	−139	−161
Pt_3Co	31	−42	42	−26

stable. The reversal of stability for Pd_3Co cannot be observed experimentally, since the calculated ΔH [Eq. (1) and Table II] is *positive*, so Pd_3Co (and similarly Pd_3Ni) is predicted to phase separate rather than to order, in accord with the observed phase-separation behaviors for Pd-Co and Pd-Ni [2].

(vi) Spin polarization can stabilize ordering over phase separation [16]: We find that in a NM description Pt_3Co has $\Delta H_{NM} > 0$ so it is predicted to phase separate, but that a strong spin-polarization effect stabilizes the ordered $L1_2$ structure, leading to $\Delta H_{FM} < 0$ in agreement with the observed ordering behavior [2]. Similarly, spin polarization stabilizes the experimentally observed [17] $L1_2$ structure of Pd_3Cr (its magnetic behavior, however, has not been experimentally examined). Hence, spin polarization not only reverses the stability of the $L1_2$ and $D0_{22}$ structures for many compounds, but it also stabilizes an ordered ($L1_2$) structure over phase separation for Pd_3Cr and Pt_3Co.

(vii) Interestingly, the ΔH for Pt_3Cr are negative in both the NM and FM cases, but the spin polarization effect gives a larger stability to the $L1_2$ structure (observed experimentally) [2]. One also notices that the ΔH are lower in the Pt alloys than in the corresponding Pd alloys. The increased stability in Pt alloys has been addressed previously in Ref. [16].

In summary, we have shown that theoretically unstable nonmagnetic structures which involve magnetic atoms and possess *large* $N(E_F)$, may be stabilized by splitting the near E_F peak in the DOS and forming a local magnetic moment with a concomitant *lowering* of $N(E_F)$ and the total energy. Therefore theoretical studies of the stability of compounds with a large value of a NM $N(E_F)$ should be carefully tested for magnetic ordering which can often change the predictions of the ground state crystal structure.

We thank Professor Alan Ardell for pointing out the fact that Pd_3Cr orders in the $L1_2$ structure. Z. W. L. and B. M. K. acknowledge the support by the University Research Funds of the University of California at Davis and San Diego Supercomputer Center for computer time. A. Z. acknowledges the DOE, the Office of Energy Research, Basic Energy Sciences, Division of Materials Science for support under Contract No. DE-AC36-83CH10093.

[1] P. Villar and L. D. Calvert, *Pearson's Handbook of Crystallographic Data for Intermetallic Phases* (ASM, Metals Park, OH, 1991).

[2] *Binary Alloy Phase Diagrams,* edited by T. B. Massalski *et al.* (ASM, Metals Park, OH, 1990).

[3] Pd_3Ti crystallizes in a hexagonal $D0_{24}$ structure as well as in an off-stoichiometric $L1_2$ structure. Pd_3Mn is observed in the $D0_{23}$ structure, which could be characterized as a combination of the $L1_2$ and $D0_{22}$ structures.

[4] (a) A. Bieber *et al.* Solid State Commun. **39**, 149 (1981); (b) **45**, 585 (1983); (c) A. Bieber and F. Gautier, Acta Metall. **34**, 2291 (1986).

[5] D. M. Nicholson *et al.,* Mater. Res. Soc. Symp. Proc. **133**, 17 (1989); **186**, 229 (1991).

[6] A. E. Carlson and P. J. Meschter, J. Mater. Res. **4**, 1060 (1989).

[7] J. Xu and A. J. Freeman, Phys. Rev. B **40**, 11 927 (1989); J. Mater. Res. **6**, 1188 (1991).

[8] N. F. Mott and H. Jones, *The Theory of the Properties of Metals and Alloys* (Clarenden Press, Oxford, 1936).

[9] W. Kohn and L. J. Sham, Phys. Rev. **140**, A1133 (1965).

[10] D. J. Singh, *Planewaves, Pseudopotentials, and the LAPW Method* (Kluwer, Boston, 1994).

[11] E. G. Moroni and T. Jarlborg, Phys. Rev. B **47**, 3255 (1993).

[12] We use the exchange-correlation potential of D. M. Ceperley and B. J. Alder, Phys. Rev. Lett. **45**, 566 (1980) as parametrized by J. P. Perdew and A. Zunger, Phys. Rev. B **23**, 5048 (1981).

[13] (a) S. Froyen, Phys. Rev. B **39**, 3168 (1989); (b) H. J. Monkhorst and J. D. Pack, *ibid.* **13**, 5188 (1976).

[14] A. Szajek, Acta Phys. Pol. A **82**, 967 (1992).

[15] S. K. Burke *et al.,* J. Magn. Magn. Mater. **15-18**, 505 (1980).

[16] Z. W. Lu, S.-H. Wei, and A. Zunger, Phys. Rev. Lett. **66**, 1753 (1991); these authors have also shown that relativistic effects can stabilize ordering over phase separation in NiPt.

[17] J. C. Huang, A. J. Ardell, and O. Ajaja, J. Mater. Sci. **23**, 1206 (1988).